

# The morphology of clusters of galaxies in eRASS1

Jeremy Sanders

*Max Planck Institute for Extraterrestrial Physics*

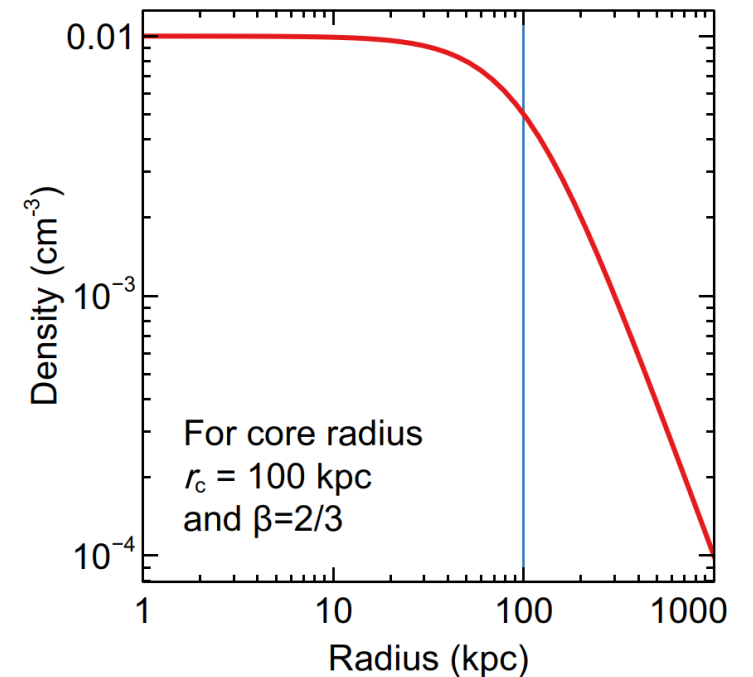
Y. E. Bahar, E. Bulbul, V. Ghirardini, A. Liu, F. Balzer, N. Clerc, J. Comparat,  
M. Kluge, F. Pacaud, M. Ramos-Ceja, T. Reiprich, X. Zhang

# Cluster morphologies

- In X-rays we are observing the dominant baryonic component of clusters of galaxies
- This hot atmosphere, the intracluster medium, ICM, is still often assumed to be spherical, with a profile following a beta model:

$$n(r) = n_0 [1 + (r/r_c)^2]^{-3\beta/2}$$

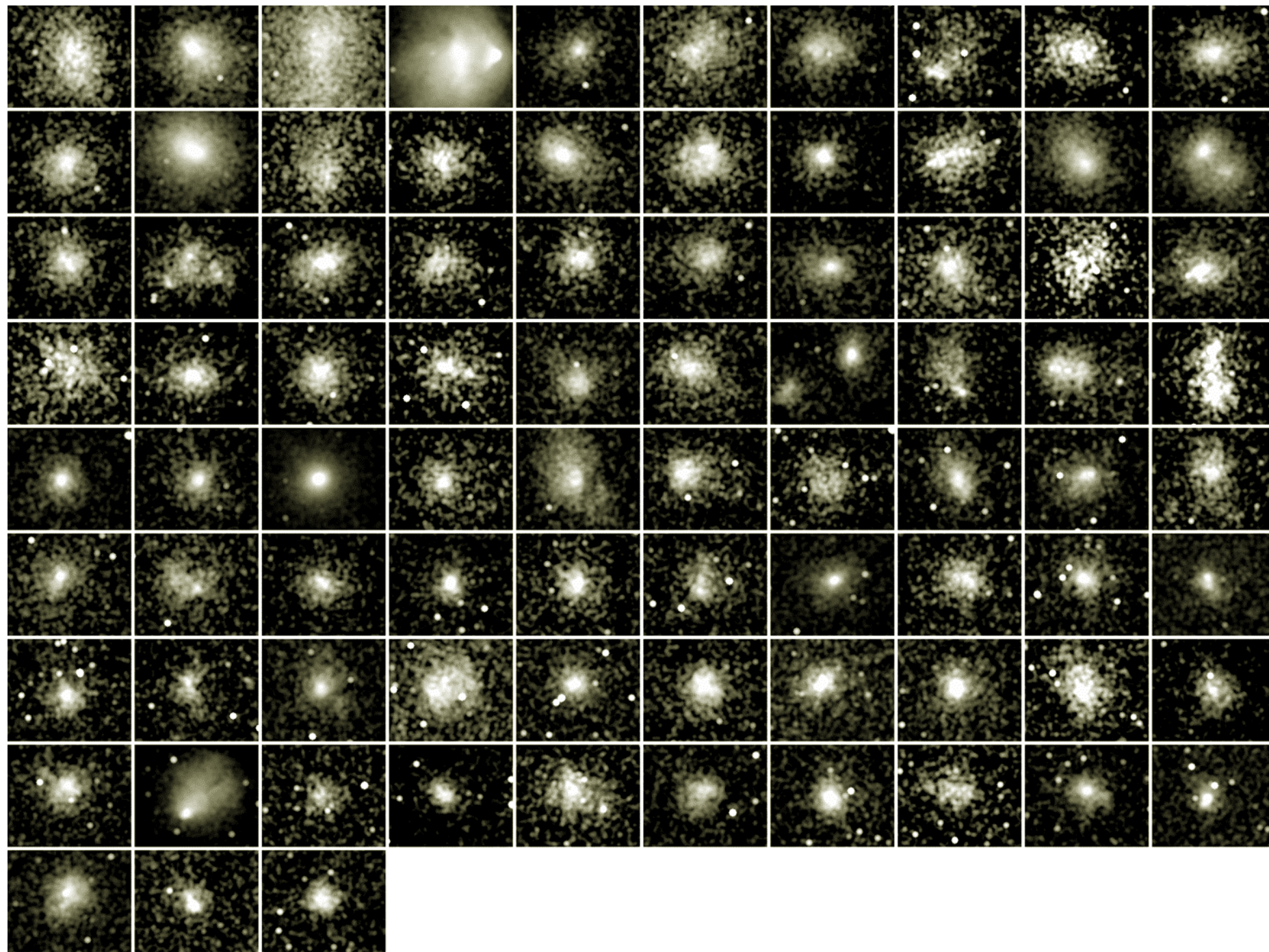
- However, that's a very simplified view of clusters



Chandra  
observations of  
clusters selected  
by the SPT  
telescope

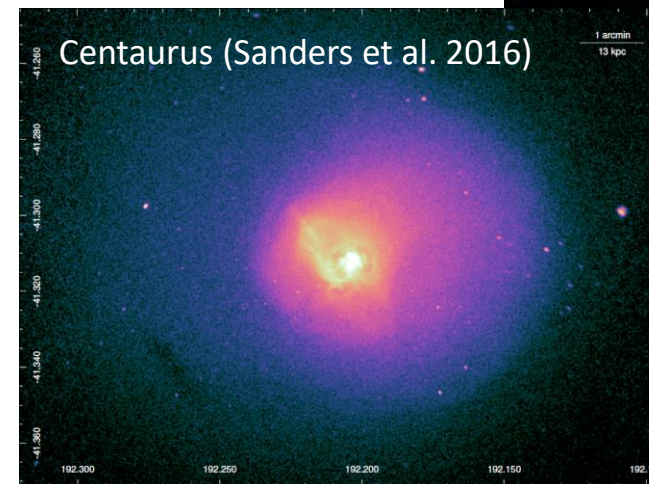
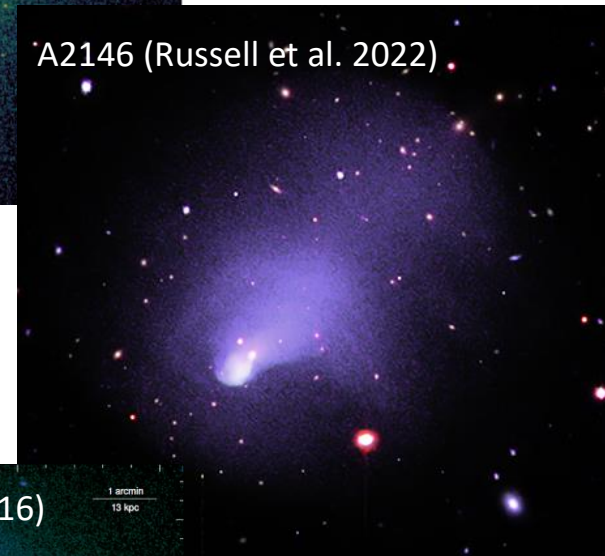
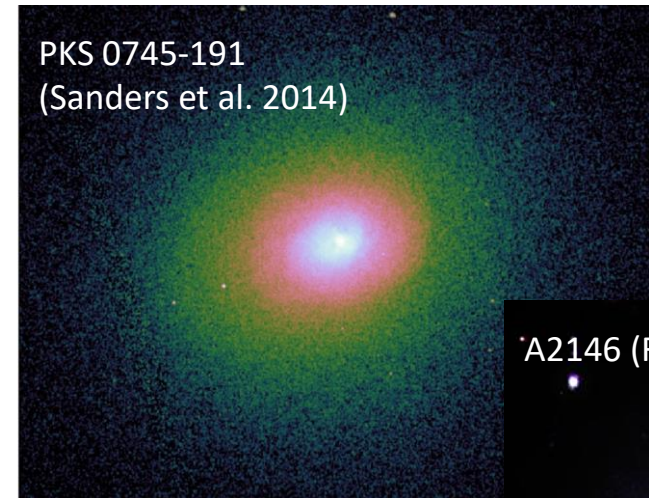
Redshift order  
(0.28 to 1.2,  
median  $\sim 0.6$ )

4.5x3.5 arcmin  
regions



# Cluster morphologies

- In particular, many clusters have a steeply peaked X-ray and density profiles – **cool core clusters** (e.g. Fabian 2012)
  - These clusters are also more likely to be relaxed and symmetric
- **Merging clusters** disturb the 2D shape of the object – see Bullet cluster (e.g. Clowe et al. 2004)
- **Minor mergers** give rise to sloshing ('cold front'; Markevitch & Vikhlinin 2007)

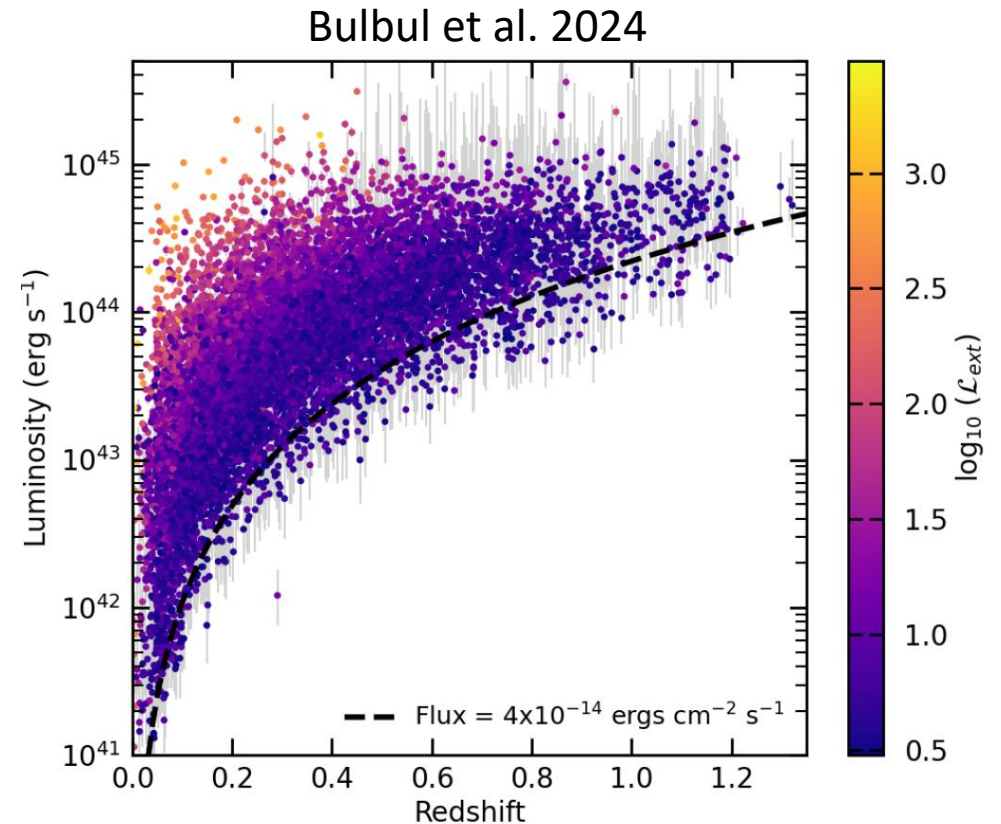


# Why are they interesting?

- Morphology is connected to **global properties** of clusters, e.g. cool core clusters have higher luminosities
- Morphology might affect **mass determinations**, if observable is affected by morphology
- We might want to study **astrophysics and evolution of clusters**, including mergers and cool cores
- Morphology can affect **how cluster is selected** in an X-ray survey

# Our cluster sample

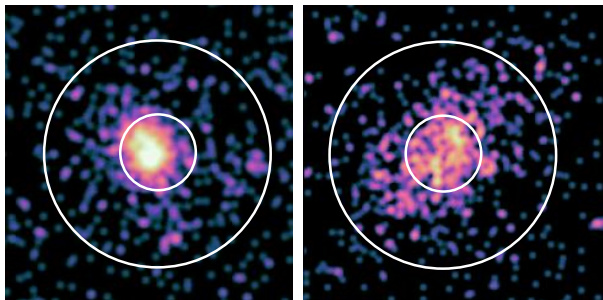
- Over 12,000 optically confirmed clusters have been found in eRASS1 (Bulbul et al. 2024)
- Spans redshifts from 0.003 to 1.32
- Masses from  $5 \times 10^{12}$  to  $2 \times 10^{15} M_{\text{sun}}$
- Largest sample of X-ray observed clusters which can be used to study morphology



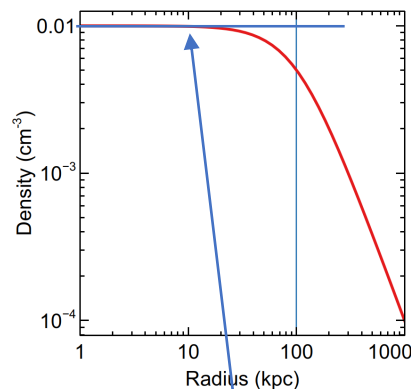
# Morphological parameters

- We can characterise cluster morphology using a number of different measurements (i.e. parameters)
- These are sensitive to different aspects of a cluster morphology and are not equivalent to each other

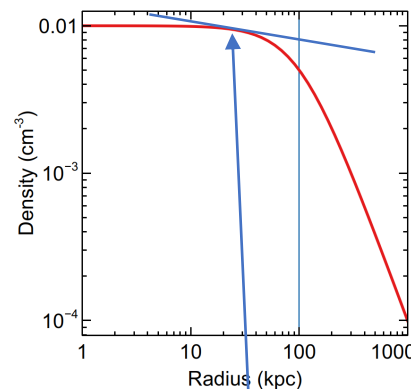
# Morphological parameters



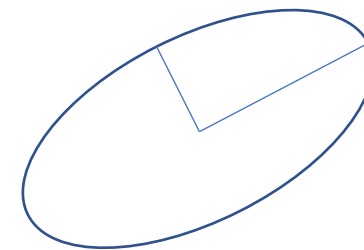
**Concentration ( $c$ ):** fraction of flux in a small vs large aperture (e.g.  $0.1R_{500} \rightarrow R_{500}$  or  $80 \rightarrow 800$  kpc)



**Central density ( $n_0$ ):** density or scaled density at some radius



**Inner slope/ Cuspsiness ( $\alpha$ )**

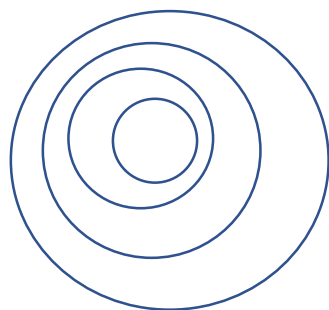


**Ellipticity ( $\epsilon=b/a$ ):** ratio of minor to major axis

Obtained by forward modelling (MBProj2D)

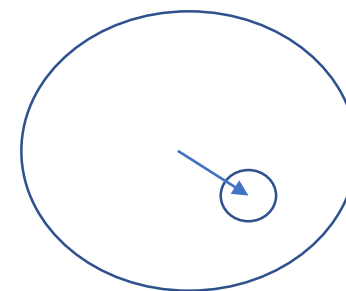
Image based – dependent on PSF+noise

**Centroid shift ( $w$ ):** variance of centroid with different apertures



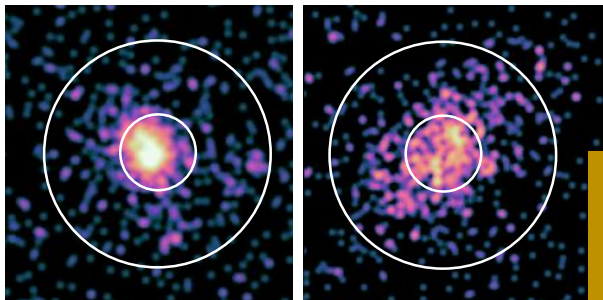
- **Photon asymmetry ( $A_{\text{phot}}$ ):** how asymmetric are photons around centre?
- **Gini coefficient ( $G$ ):** economic measure applied to measure how peaky the cluster is
- **Power ratios ( $P_{10}, P_{20} \dots$ ):** decompose clusters into multipoles and calculate power from each relative to 0 order

**Fit-peak offset ( $F$ ):** offset between cluster fit position and X-ray peak

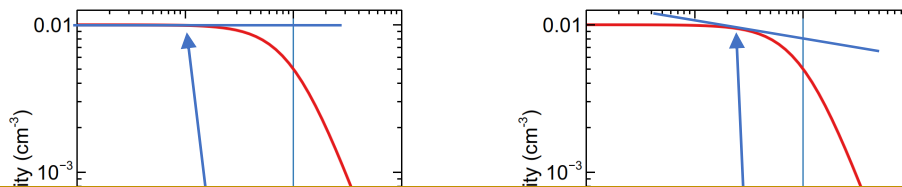




# Morphological parameters



**Concentration ( $c$ ):** fraction of flu in a small vs large aperture (e.g.  $0.1R_{500} \rightarrow R_{500}$  or  $80 \rightarrow 800$  kpc)



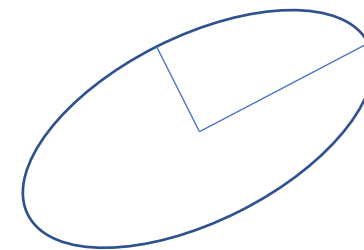
However:

Several of these parameters depend on the choice of the centre of the cluster!

If so, we both fit for the centre with a global model, or use the X-ray peak (denoted \*)

And, for some we measure at fixed physical radii and scaled radii (relative to  $R_{500}$ )

- **Power ratios ( $P_{10}, P_{20} \dots$ ):** decompose clusters into multipoles and calculate power from each relative to 0 order



**Ellipticity ( $\epsilon=b/a$ ):** ratio of minor to major axis

Obtained by forward modelling (MBProj2D)

**Fit-peak offset ( $F$ ):** offset between cluster fit position and X-ray peak

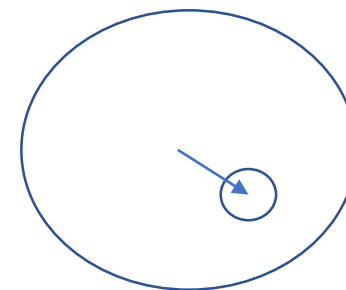
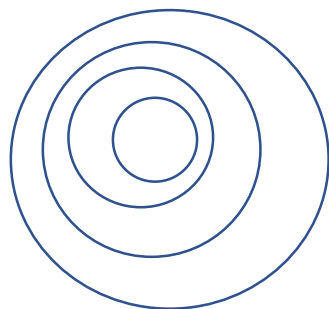
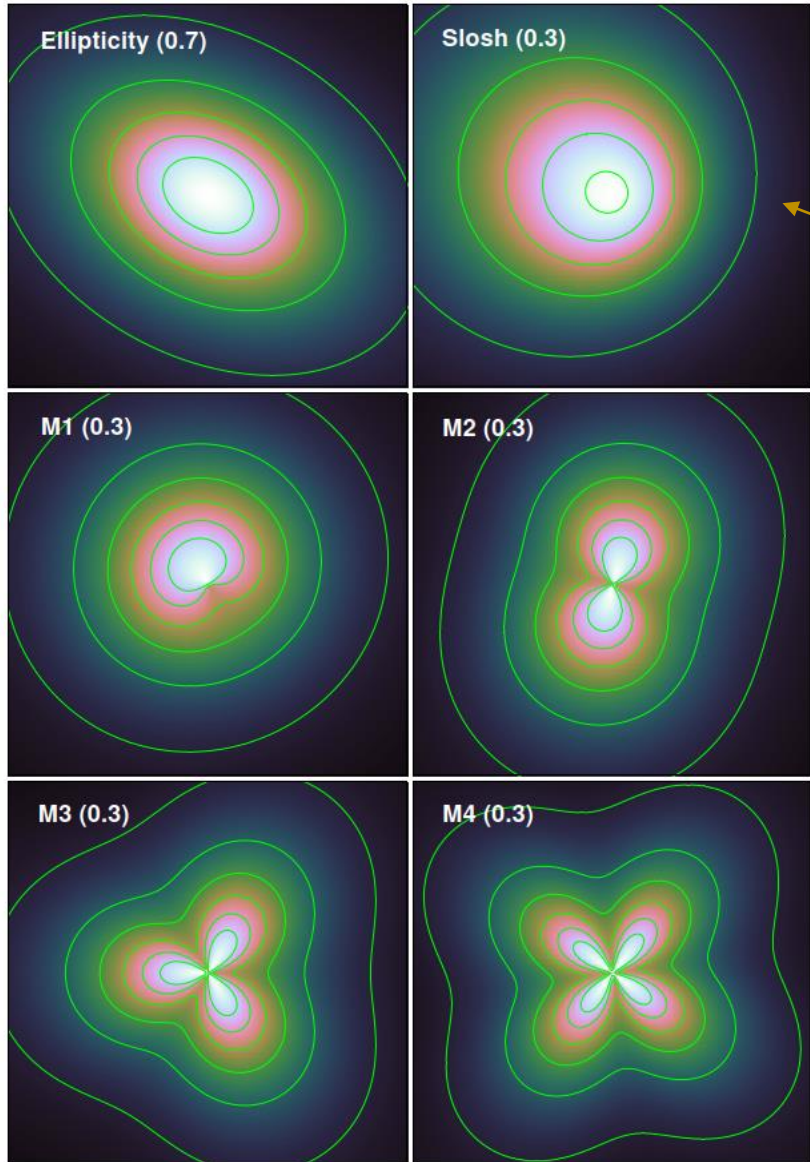


Image based – dependent on PSF+noise

**Centroid shift ( $w$ ):** variance of centroid with different apertures



# New forward-modelled parameters



Introduce new forward-modelled parameters for 2D shape

- **Slosh ( $H$ )**: looks like a sloshing cluster, where

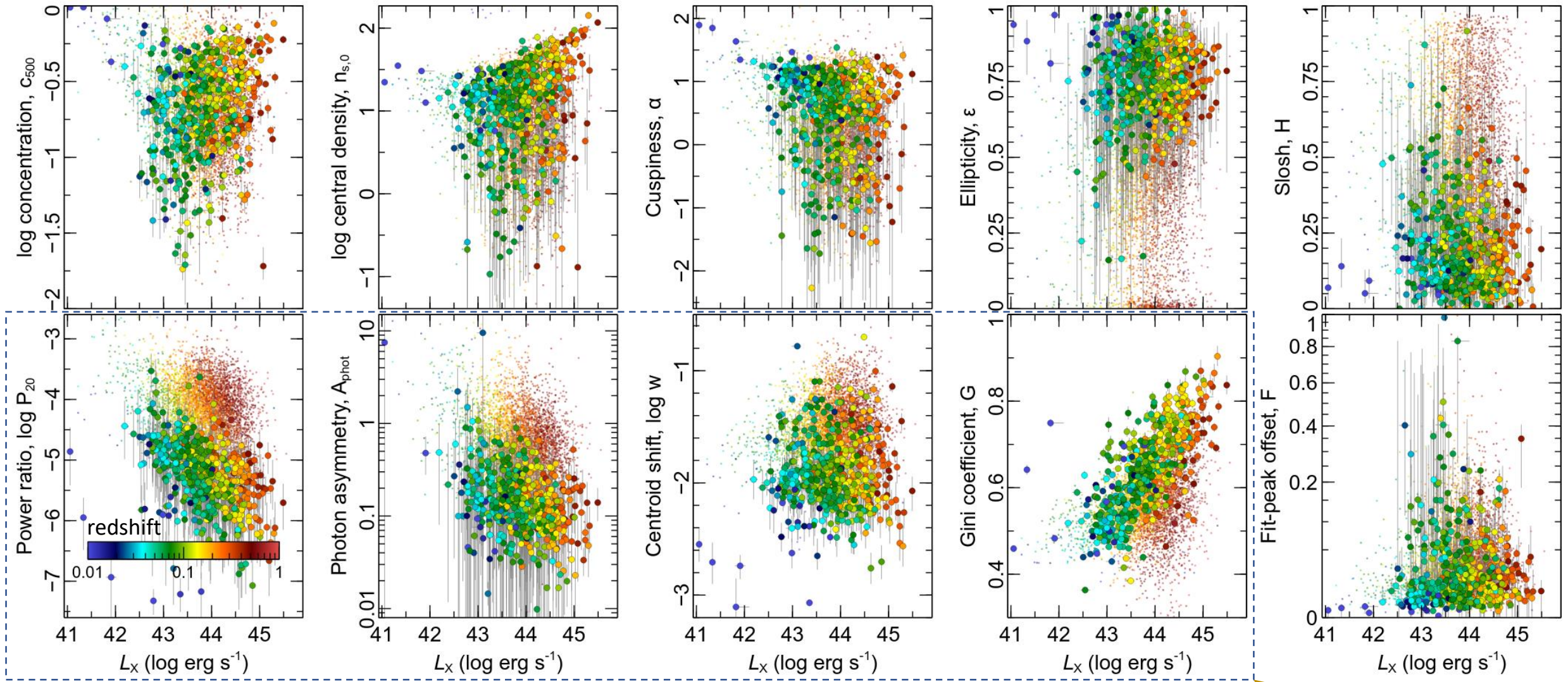
$$S'(r, \theta) = A(H) S(r [1 + H \cos(\theta + \theta_0)])$$

- **Multipole magnitude ( $M_m$ )** – similar to power ratios – where

$$S'(r, \theta) = [1 + M_m \sin(m\theta + \theta_0)] S(r)$$

for  $m = 1-4$

# Results: parameters as function of $L_x$



Subset of parameters, where big markers have >300 counts and small points have >25 counts

Markers coloured by redshift

Image-derived quantities show large systematics related to number of counts

# Example clusters

Clusters with  $\sim 1000$  counts

Shown are:

*Redshift*

*Log central density*

*Log concentration*

*Ellipticity*

*Slosh*

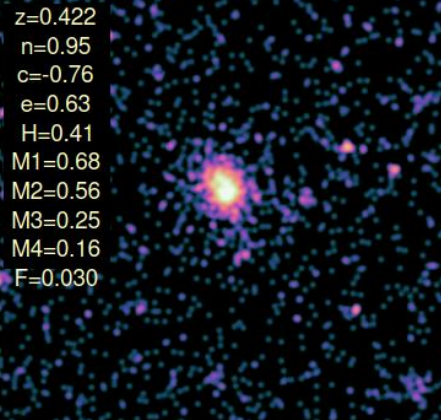
*Multipole magnitudes*

*Peak-fit offset*

Catalogue contains 29 measurements for each of the 12,000 clusters in the sample

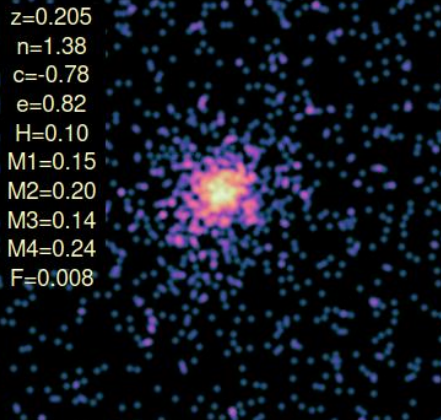
1eRASS J043817.8-541917

$z=0.422$   
 $n=0.95$   
 $c=-0.76$   
 $e=0.63$   
 $H=0.41$   
 $M1=0.68$   
 $M2=0.56$   
 $M3=0.25$   
 $M4=0.16$   
 $F=0.030$



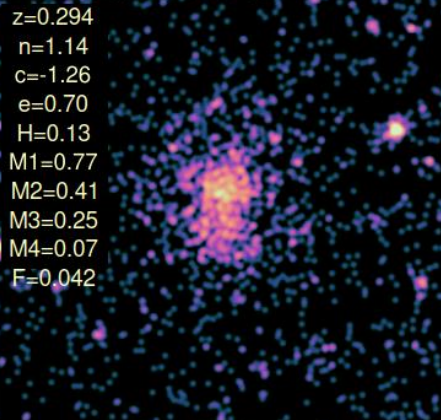
1eRASS J051016.7-451911

$z=0.205$   
 $n=1.38$   
 $c=-0.78$   
 $e=0.82$   
 $H=0.10$   
 $M1=0.15$   
 $M2=0.20$   
 $M3=0.14$   
 $M4=0.24$   
 $F=0.008$



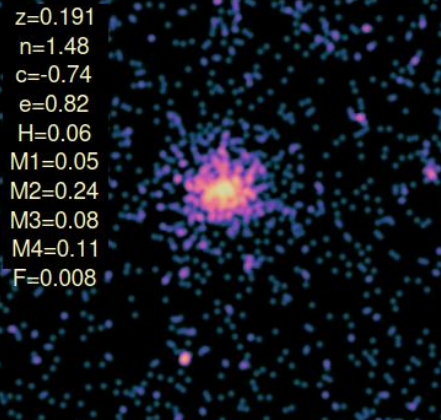
1eRASS J051636.6-543031

$z=0.294$   
 $n=1.14$   
 $c=-1.26$   
 $e=0.70$   
 $H=0.13$   
 $M1=0.77$   
 $M2=0.41$   
 $M3=0.25$   
 $M4=0.07$   
 $F=0.042$



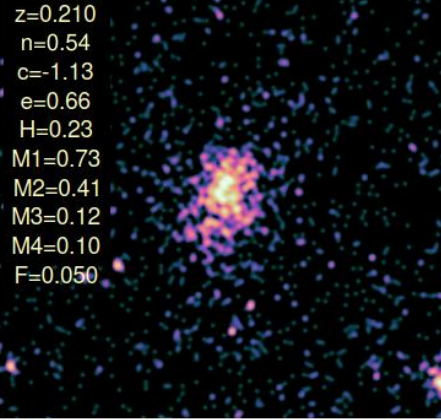
1eRASS J052548.6-471511

$z=0.191$   
 $n=1.48$   
 $c=-0.74$   
 $e=0.82$   
 $H=0.06$   
 $M1=0.05$   
 $M2=0.24$   
 $M3=0.08$   
 $M4=0.11$   
 $F=0.008$



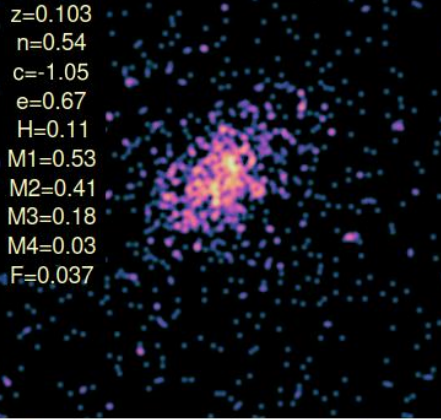
1eRASS J053128.2-751032

$z=0.210$   
 $n=0.54$   
 $c=-1.13$   
 $e=0.66$   
 $H=0.23$   
 $M1=0.73$   
 $M2=0.41$   
 $M3=0.12$   
 $M4=0.10$   
 $F=0.050$



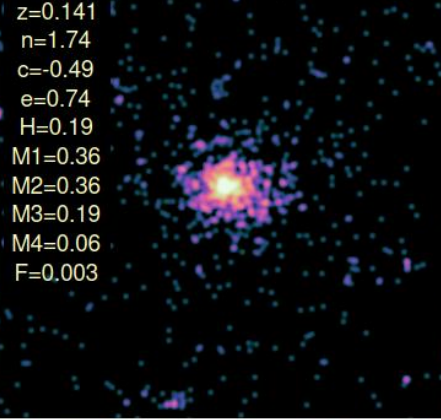
1eRASS J055252.8-210407

$z=0.103$   
 $n=0.54$   
 $c=-1.05$   
 $e=0.67$   
 $H=0.11$   
 $M1=0.53$   
 $M2=0.41$   
 $M3=0.18$   
 $M4=0.03$   
 $F=0.037$



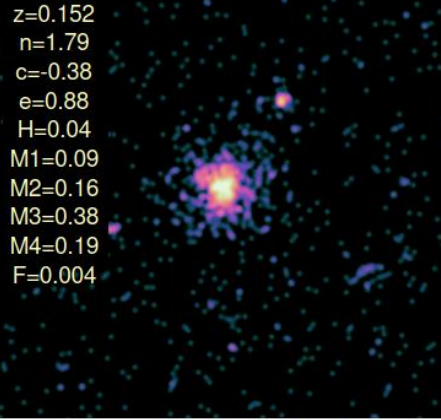
1eRASS J060554.1-351809

$z=0.141$   
 $n=1.74$   
 $c=-0.49$   
 $e=0.74$   
 $H=0.19$   
 $M1=0.36$   
 $M2=0.36$   
 $M3=0.19$   
 $M4=0.06$   
 $F=0.003$



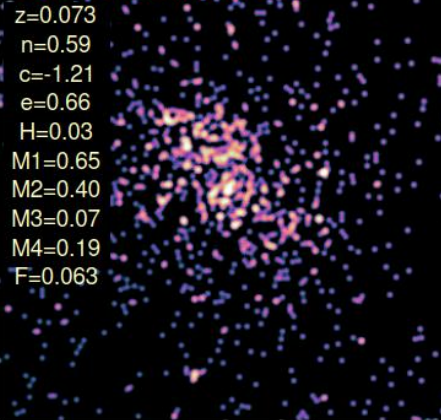
1eRASS J124009.9-482612

$z=0.152$   
 $n=1.79$   
 $c=-0.38$   
 $e=0.88$   
 $H=0.04$   
 $M1=0.09$   
 $M2=0.16$   
 $M3=0.38$   
 $M4=0.19$   
 $F=0.004$



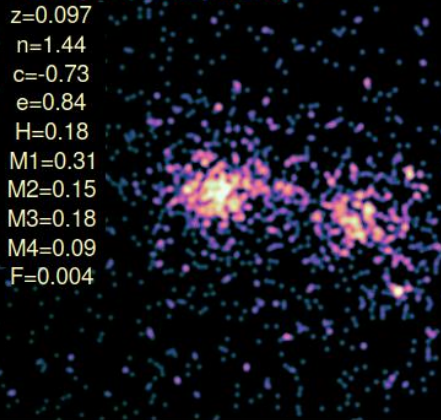
1eRASS J124116.4+183310

$z=0.073$   
 $n=0.59$   
 $c=-1.21$   
 $e=0.66$   
 $H=0.03$   
 $M1=0.65$   
 $M2=0.40$   
 $M3=0.07$   
 $M4=0.19$   
 $F=0.063$



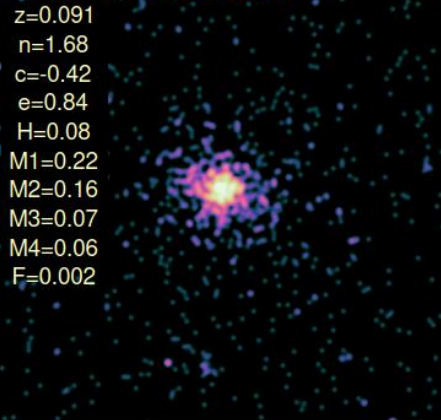
1eRASS J140755.5-505938

$z=0.097$   
 $n=1.44$   
 $c=-0.73$   
 $e=0.84$   
 $H=0.18$   
 $M1=0.31$   
 $M2=0.15$   
 $M3=0.18$   
 $M4=0.09$   
 $F=0.004$



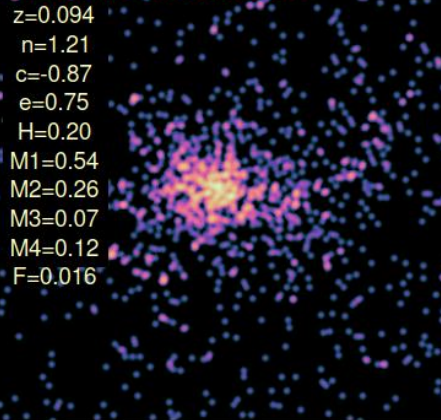
1eRASS J155821.9-140957

$z=0.091$   
 $n=1.68$   
 $c=-0.42$   
 $e=0.84$   
 $H=0.08$   
 $M1=0.22$   
 $M2=0.16$   
 $M3=0.07$   
 $M4=0.06$   
 $F=0.002$



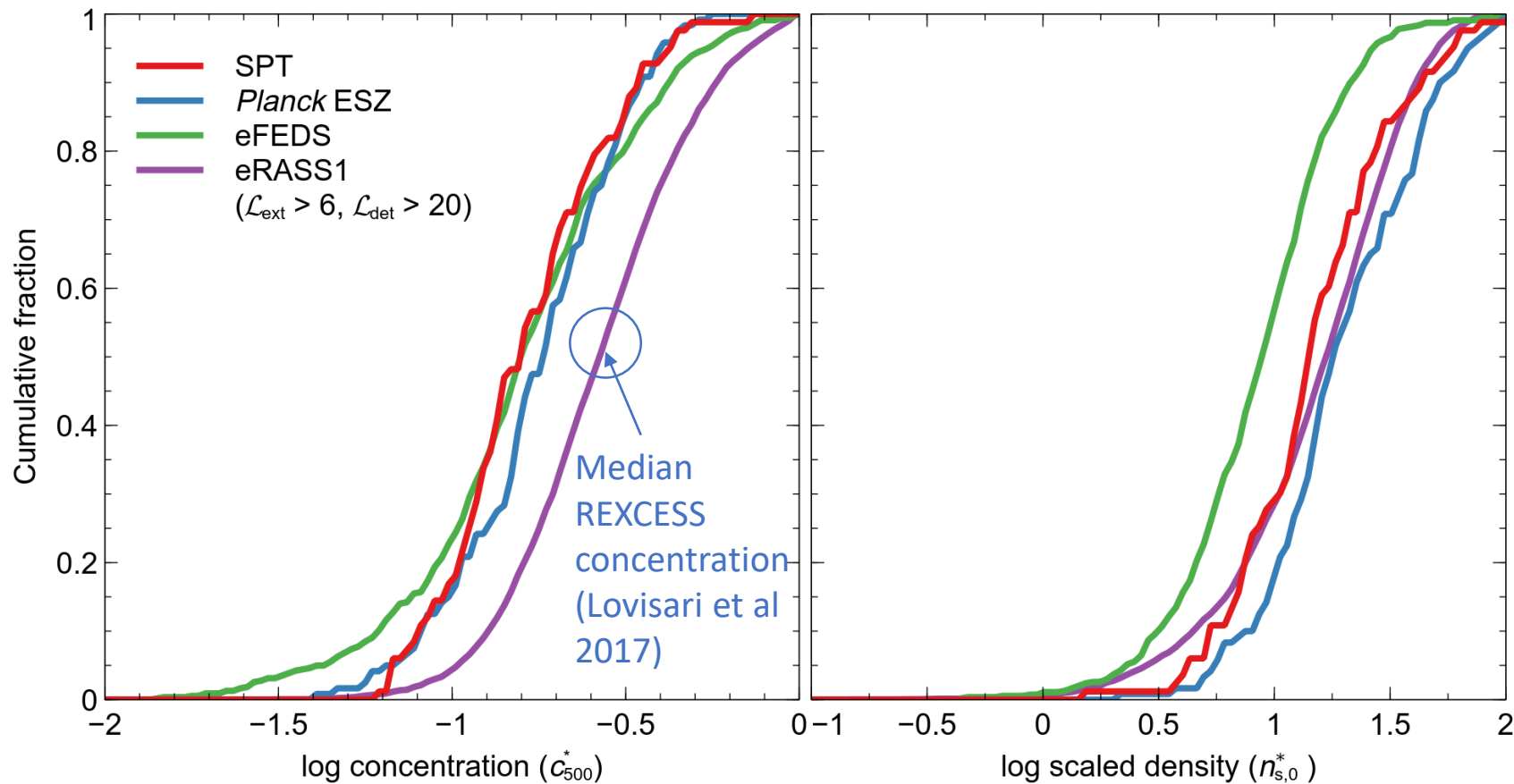
1eRASS J224956.6-642532

$z=0.094$   
 $n=1.21$   
 $c=-0.87$   
 $e=0.75$   
 $H=0.20$   
 $M1=0.54$   
 $M2=0.26$   
 $M3=0.07$   
 $M4=0.12$   
 $F=0.016$



# Comparisons with other samples

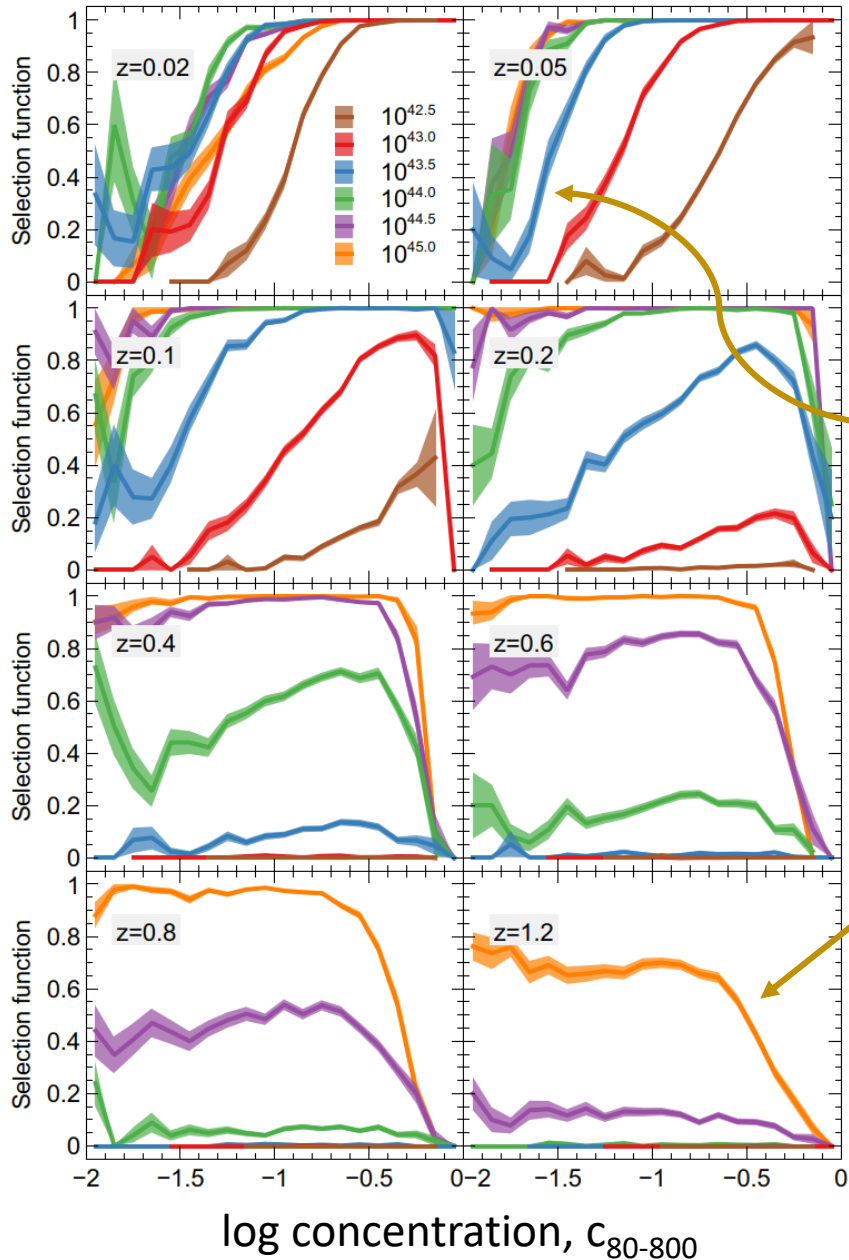
There is reasonable agreement on individual objects with previous measurements, however samples differ...



- Comparisons with
  - Planck-selected ESZ sample (Lovisari et al 2017)
  - SPT-selected sample (Bleem et al. 2015)
  - eROSITA-selected eFEDS sample (Liu et al. 2022), measured by Ghirardini et al. (2022)
- eRASS1 clusters more concentrated than the other samples, but have similar central density to SPT and Planck clusters

Selection and which subset of cluster population studied ( $z/M/L_x$ ) is important.

# Cluster selection is important

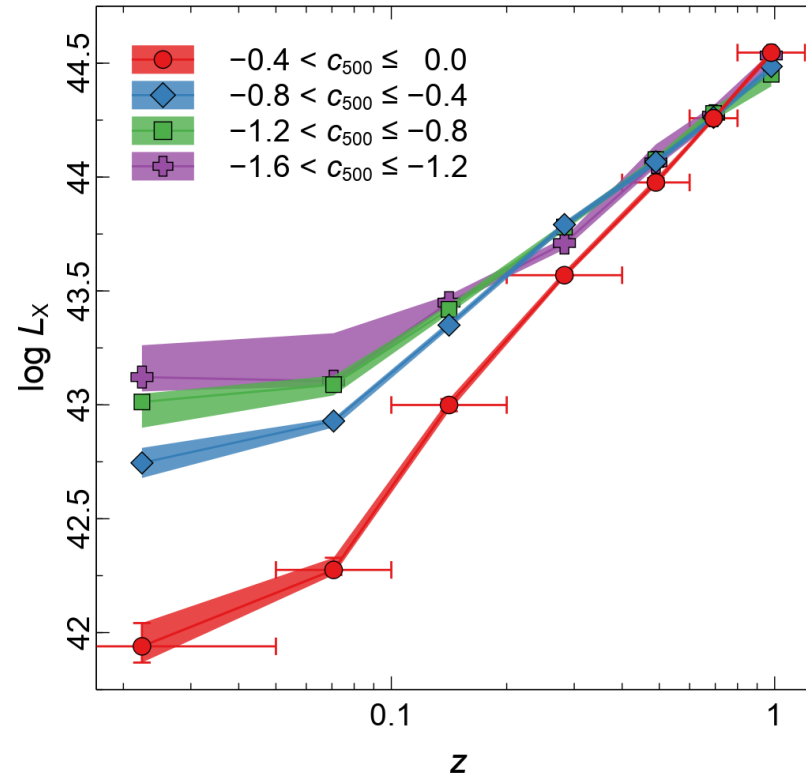


Selection function obtained from simulations, showing probability of detecting a cluster with the properties listed

Miss low concentration objects at low redshift

Miss high concentration objects at high redshift

Luminosities of clusters in bins of concentration and redshift



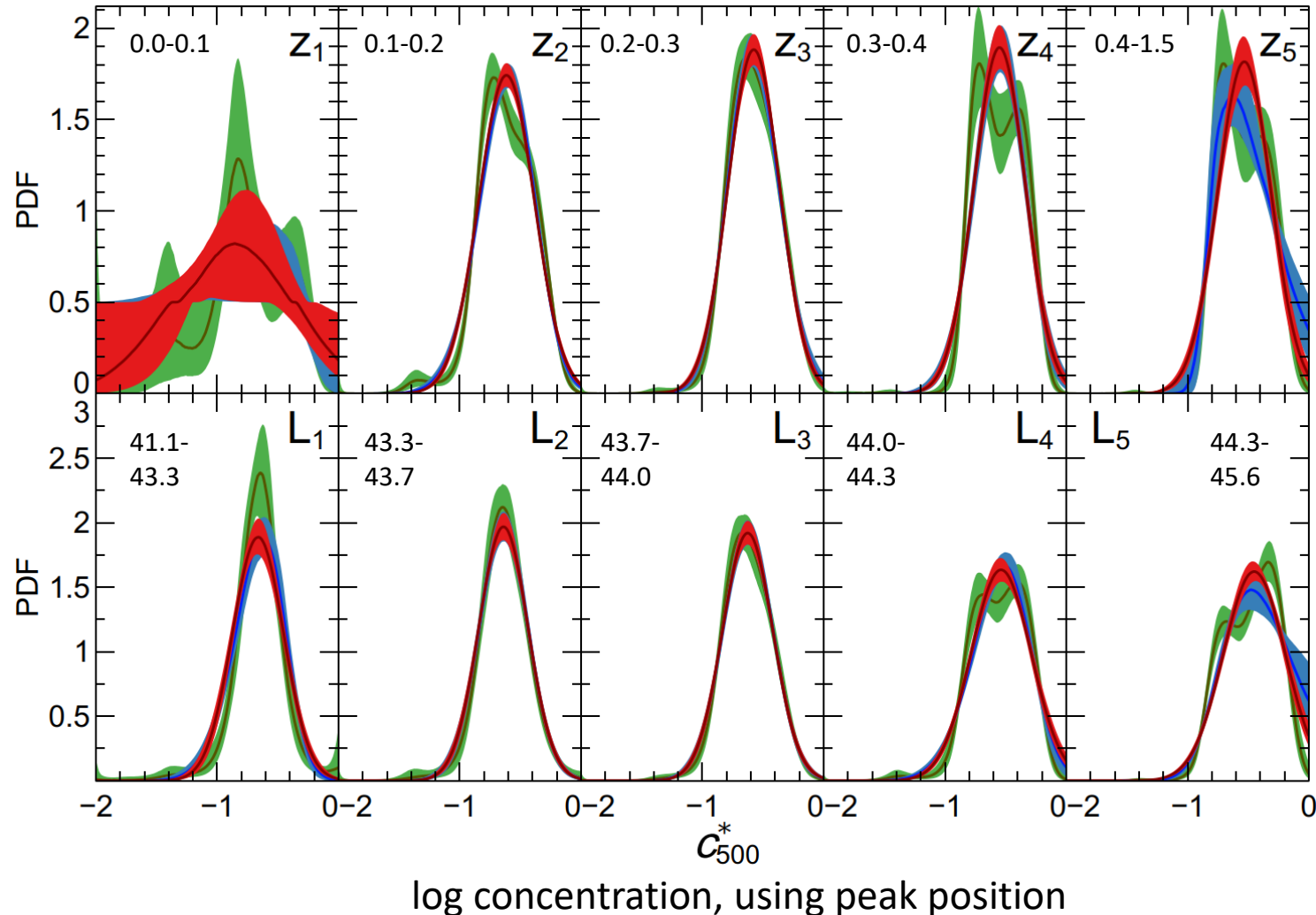
Low concentration objects have higher  $L_x$  at low  $z$ , and the opposite at high  $z$

# Modelling the distributions

Preliminary!

To properly understand the distributions, we have constructed a Bayesian model including the selection function and mass function of clusters

Measure distributions in redshift and X-ray luminosity bins, here for normal, skew and interpolated distributions

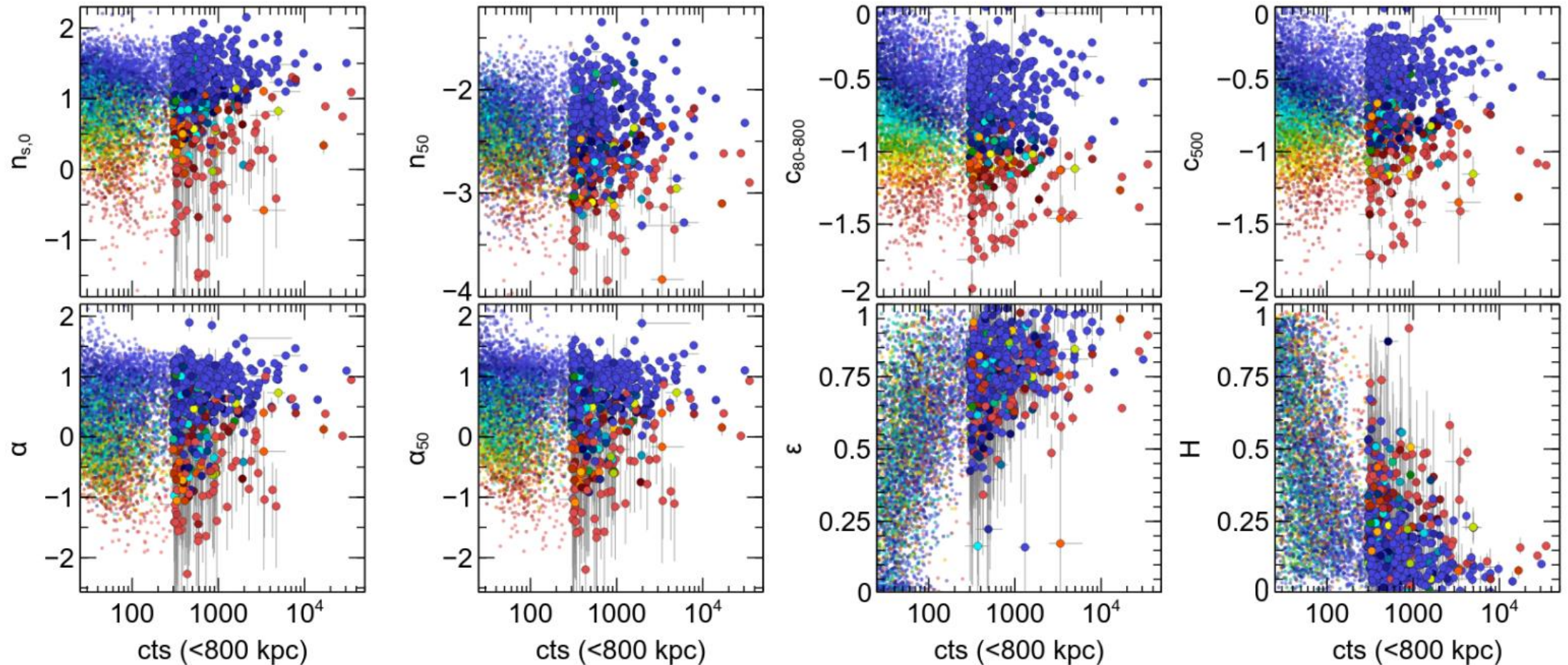


Normal distribution is statistically preferred in all these bins.

Not the case for all other parameters...

Evolution coming soon...

# Identifying relaxed systems



We fit a two-component Gaussian Mixture Model to a set of forward-modelled parameters.

Blue= relaxed  
Red = unrelaxed

Model prefers 3/4 of objects in a 'relaxed' component and 1/4 in an 'unrelaxed' component



# Conclusions

- Measured morphological properties of >12000 clusters
- Reasonable agreement with other measurements of the same clusters
- Forward modelled parameters less subject to bias and noise than image-derived parameters
- eRASS1 clusters are more concentrated than those found by SZ surveys
- Majority of systems classified as relaxed
- We are modelling the distribution of parameters and evolution, taking into account the selection functions